

SpikePingpong: High-Frequency Spike Vision-based Robot Learning for Precise Striking in Table Tennis Game

Hao Wang^{1,2*}, Chengkai Hou^{1*}, Xianglong Li^{2*}
 Yankai Fu¹, Chenxuan Li¹, Ning Chen¹, Gaole Dai¹, Jiaming Liu¹
 Tiejun Huang^{1,2}, Shanghang Zhang^{1,2†}
¹Peking University, Beijing, China
²Beijing Academy of Artificial Intelligence (BAAI), Beijing, China
 haowang@stu.pku.edu.cn

Abstract

Learning to control high-speed objects in the real world remains a challenging frontier in robotics. Table tennis serves as an ideal testbed for this problem, demanding both rapid interception of fast-moving balls and precise adjustment of their trajectories. This task presents two fundamental challenges: it requires a high-precision vision system capable of accurately predicting ball trajectories, and it necessitates intelligent strategic planning to ensure precise ball placement to target regions. The dynamic nature of table tennis, coupled with its real-time response requirements, makes it particularly well-suited for advancing robotic control capabilities in fast-paced, precision-critical domains. In this paper, we present *SpikePingpong*, a novel system that integrates spike-based vision with imitation learning for high-precision robotic table tennis. Our approach introduces two key attempts that directly address the aforementioned challenges: SONIC, a spike camera-based module that achieves millimeter-level precision in ball-racket contact prediction by compensating for real-world uncertainties such as air resistance and friction; and IMPACT, a strategic planning module that enables accurate ball placement to targeted table regions. The system harnesses a 20 kHz spike camera for high-temporal resolution ball tracking, combined with efficient neural network models for real-time trajectory correction and stroke planning. Experimental results demonstrate that SpikePingpong achieves a remarkable 91% success rate for 30 cm accuracy target area and 71% in the more challenging 20 cm accuracy task, surpassing previous state-of-the-art approaches by 38% and 37% respectively. These significant performance improvements enable the robust implementation of sophisticated tactical gameplay strategies, providing a new research perspective for robotic control in high-speed dynamic tasks.

1 Introduction

Current research in robot learning primarily focuses on manipulation tasks involving static or slow-moving objects, such as folding clothes [5, 49], pouring water [48, 28], and grasping arbitrary items [46, 42]. While these achievements represent significant progress, they address scenarios with relatively simple dynamics. Yet, the real world is replete with dynamic scenarios involving high-speed moving objects that demand rapid perception and precise control, from catching falling

*Equal contribution

†Corresponding author

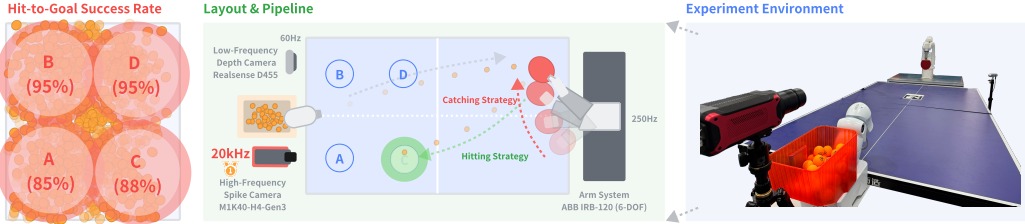


Figure 1: **Overview of SpikePingpong.** Our framework decomposes table tennis into two specialized phases: (1) the interception phase using SONIC, which leverages spike camera data to accurately intercept the incoming ball, and (2) the hitting phase employing IMPACT, which uses imitation learning to direct the ball to specified target locations. Experiments demonstrate 91% success rate for primary accuracy zones and 71% for high-precision targeting across four distinct regions.

items [54] and intercepting projectiles [36] to navigating through crowded environments with moving obstacles [17]. These challenging contexts require robots to process information and react at speeds approaching or even surpassing human capabilities, thereby posing a critical frontier for advancing robotic learning beyond simplified, low-dynamic environments. To address these challenges, we explore the control of high-speed moving objects, with table tennis serving as an ideal testbed. This dynamic sport presents unique challenges beyond traditional robotics applications, requiring millisecond-level timing accuracy and millimeter-level spatial precision.

When tackling high-speed dynamic tasks like robotic table tennis, existing approaches can be broadly categorized into control-based methods and learning-based methods, each with its distinct limitations in this challenging domain. Control-based approaches [2, 35, 53, 43, 50] rely on precise physical modeling and predefined motion planning strategies. These methods benefit from mathematical rigor and computational efficiency but struggle to cope with real-world complexities, as they require precise calibration and physical parameters that make them brittle to environmental variations. Furthermore, they lack the ability to adaptively adjust strategies in response to varying ball trajectories or unexpected disturbances. Learning-based approaches [34, 1, 11, 16, 13, 56], particularly reinforcement learning techniques, offer greater theoretical adaptability. However, they often suffer from the persistent sim-to-real gap, where policies trained in simulation perform poorly in physical systems. This is particularly pronounced in table tennis, where subtle factors like ball spin and contact dynamics significantly impact performance. Most similar to our work, GoalsEye [13] employs iterative imitation learning but achieves only modest accuracy in ball placement. In contrast, our imitation learning approach circumvents the sim-to-real gap inherent in reinforcement learning while providing adaptive capabilities lacking in control-based methods, ultimately achieving significantly higher precision control than existing systems.

In this paper, we propose **SpikePingpong**, a high-precision robotic table tennis system integrating spike-based vision and advanced control techniques as illustrated in Figure 1. Our approach decomposes the complex task of table tennis into two distinct phases with specialized technical solutions: the interception phase and the hitting phase. For interception, we introduce SONIC (Spike-Oriented Neural Improvement Calibrator), a module designed to overcome the inherent limitations of conventional control approaches. SONIC leverages a lightweight neural prediction framework trained on high-fidelity spike camera data to precisely forecast the deviation between racket center and optimal ball contact position. This innovation effectively addresses unavoidable inaccuracies in physical models caused by environmental variables and spin dynamics that are typically difficult to detect and model precisely. For hitting, our IMPACT (Imitation-based Motion Planning And Control Technology) module learns striking actions from demonstrations that map incoming ball trajectories to effective racket movements, enabling control of the ball’s landing position with remarkable precision. In summary, our contributions are as follows:

- We propose SpikePingpong, a novel robot learning framework that decomposes the complex table tennis task into specialized interception and hitting phases, addressing the limitations of both traditional control-based and learning-based approaches.
- We introduce a comprehensive neural control system combining SONIC, a calibration system for precise ball-racket interaction prediction, and IMPACT, an imitation learning

framework that captures expert striking strategies through demonstrations to enable precise control over ball landing positions.

- Experimental results demonstrate that SpikePingpong achieves a remarkable 91% success rate for 30cm accuracy zones and 71% for high-precision 20cm targeting across four distinct target regions, surpassing previous state-of-the-art approaches by 38% and 37% respectively.

2 Related Work

2.1 Agile Policy Learning

Agile policy learning addresses the challenge of generating fast, adaptive, and robust behaviors in highly dynamic environments. It has been widely studied across various domains such as autonomous driving [38, 41, 33, 4, 39], legged locomotion [37, 44, 18, 57], humanoid skills [19, 6, 20, 52] and dynamic manipulation tasks like throwing and catching [54, 21, 24, 22, 27]. These tasks require policies capable of maintaining high inference frequencies, handling disturbances, and generalizing across a wide range of conditions. Perception plays a critical role in enabling robots to adapt to environmental changes [47] and to understand the dynamic interaction between objects and agents [51, 25, 15]. When tracking fast-moving objects, systems often rely on high-speed motion capture setups [32]. However, in table tennis scenarios, the high speed and abrupt motion of the ball cause significant motion blur with standard RGB cameras, leading to inaccurate position estimates and trajectory predictions. Unlike previous systems that rely on multi-camera setups, our SONIC module utilizes a neuromorphic spike camera to capture high-temporal-resolution data of ball-racket interactions. This enables us to measure and predict the deviation between expected and actual contact points, training a neural network that compensates for systematic errors without complex physical modeling. This approach significantly improves interception accuracy in our high-speed robotic table tennis system.

2.2 Robotic Table Tennis

Robotic table tennis has long served as a benchmark task in robotics due to its requirement for real-time perception, prediction, planning, and control. Ever since Billingsley initiated the first robot table tennis competition in 1983 [7], the task has attracted continuous attention from the research community. The existing approaches can be broadly categorized into two groups: control-based methods and learning-based methods. **Control-based approaches** [2, 35, 53, 43, 50] rely on mathematical modeling and predefined control strategies. These methods typically follow a perception-prediction-control pipeline: detecting the ball, predicting a virtual hitting point [30, 31], and generating joint-space trajectories to reach this point [23, 26]. While these approaches benefit from mathematical rigor, they often require precise calibration and struggle with adapting to environmental variations or unexpected ball dynamics. **Learning-based methods**, particularly reinforcement learning and imitation learning, have gained prominence in recent years. Reinforcement learning approaches [9, 45, 16, 56] directly map sensory inputs to motor commands, offering greater adaptability. Abeyruwan et al. [1] proposed an iterative sim-to-real method, while D’Aronco et al. [11] presented a system addressing perception latency for transfer. Most similar to our approach, GoalsEye [13] employs imitation learning for table tennis through demonstrations and self-supervised practice, but its reliance on sim2real transfer limits its performance. Our work takes a fundamentally different approach by employing direct imitation learning exclusively in the physical world and leveraging spike cameras for enhanced perception, achieving more precise target control capabilities without simulation limitations.

3 Method

In this section, we present our robotic table tennis framework SpikePingpong, consisting of three integrated components as shown in Figure 2. First, we employ a physics-based trajectory prediction system using a low-frequency RGB-D camera to estimate the ball’s initial hittable position. Second, we introduce SONIC (Spike-Oriented Neural Improvement Calibrator), which leverages neuromorphic vision to refine hittable position predictions by compensating for real-world physical effects. Finally, our IMPACT (Imitation-based Motion Planning And Control Technology) module generates strategic hitting motions based on visual input and landing information, enabling tactical control over

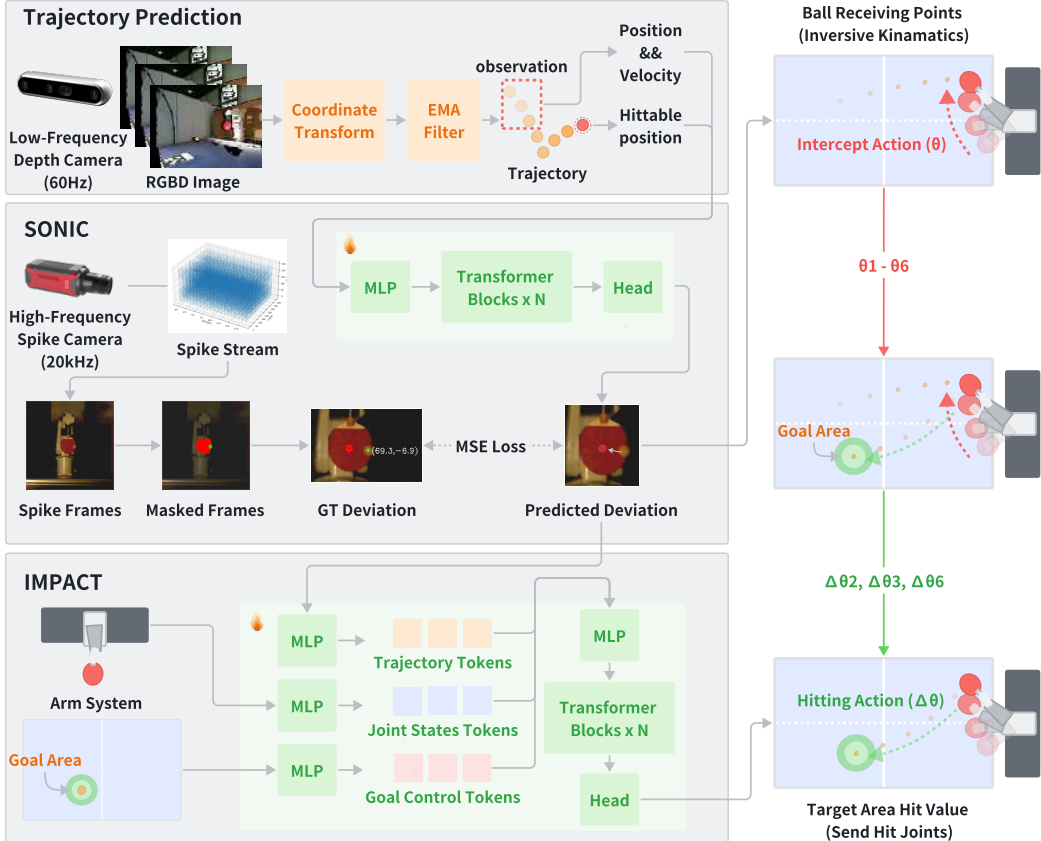


Figure 2: **Framework of SpikePingpong.** Our system integrates three key components: (1) initial trajectory prediction using RGB-D camera data, (2) SONIC module for refined hittable position estimation through neuromorphic vision, and (3) IMPACT module for strategic motion planning and control. This comprehensive pipeline enables precise ball interception and tactical return placement.

return placement. This pipeline progresses from basic trajectory estimation to precise interception and strategic gameplay execution.

3.1 Ball Detection and Trajectory Prediction

Ball Detection. In high-speed robotic table tennis, we employ YOLOv4-tiny [8] for its computational efficiency, achieving detection frequencies up to 150 Hz. Our two-phase training strategy involves initial training on public datasets (Roboflow [3], TT2 [12], and Ping Pong Detection [40]), followed by targeted fine-tuning on difficult samples with higher weights. Using an Intel RealSense D455 RGB-D camera, our system achieves over 99.8% detection accuracy, transforming 2D detections into 3D world coordinates for precise trajectory estimation and timely ball interaction.

Ball Trajectory Prediction. Table tennis balls can reach velocities of 2-30m/s after being struck, requiring robotic systems to accurately predict their trajectories for successful interception. We propose a physics-based approach that enables our robotic arm to anticipate the ball’s path and position itself optimally for interception. Our prediction model first employs Exponential Moving Average filtering to obtain reliable estimates of the ball’s current position (x, y, z) and velocity (v_x, v_y, v_z) in the world coordinate system. These filtered state estimates serve as input to our physics model, which outputs the predicted hittable position ($x_{\text{hit}}, y_{\text{hit}}, z_{\text{hit}}$) and corresponding velocity ($v_x^{\text{hit}}, v_y^{\text{hit}}, v_z^{\text{hit}}$). With gravitational acceleration g , we calculate the time t required for the ball to reach the predetermined interception plane at y_{hit} : $t = \frac{y_{\text{hit}} - y}{v_y}$. Using this time value, we predict the x-coordinate at interception: $x_{\text{hit}} = x + v_x \cdot t$. If x_{hit} falls outside the robot’s operational workspace, the ball is classified as unhittable. For the z-coordinate prediction, we consider two scenarios:

- **Direct trajectory:** If the ball doesn't contact the table before reaching y_{hit} , we compute $z_{\text{hit}} = z + v_z \cdot t + \frac{1}{2}gt^2$. When $z_{\text{hit}} > h_{\text{table}}$, no rebound occurs.
- **Rebound trajectory:** If the ball impacts the table, we calculate the rebound time t_{rb} by solving: $z + v_z \cdot t_{\text{rb}} + \frac{1}{2}gt_{\text{rb}}^2 = h_{\text{table}}$. We then determine the impact velocity $v_{z,\text{in}}$ and post-rebound velocity $v_{z,\text{out}}$ using:

$$v_{z,\text{in}} = -\sqrt{-2g(z - h_{\text{table}}) + v_z^2}, \quad (1)$$

$$v_{z,\text{out}} = -e \cdot v_{z,\text{in}}. \quad (2)$$

where e represents the coefficient of restitution. The system further evaluates potential secondary rebounds to determine the final z_{hit} and v_z^{hit} .

While our model effectively predicts trajectories under ideal conditions—assuming constant v_x, v_y velocity, precise position detection, and standard gravitational acceleration g —real-world scenarios introduce significant deviations from these theoretical assumptions. In the following section, we describe our implementation of a high-frame-rate Spike camera system that compensates for these prediction errors, substantially enhancing the accuracy of our trajectory estimation framework.

3.2 SONIC: Spike-Oriented Neural Improvement Calibrator

Our physics-based prediction approach necessarily simplifies real-world conditions by neglecting air resistance, spin effects, and assuming constant gravitational acceleration—idealizations that introduce systematic prediction errors in practice. To address these challenges, we develop **SONIC** (Spike-Oriented Neural Improvement Calibrator), employ a neural network to predict the discrepancy between the model's predicted hittable position and the real-world hittable position.

The SONIC methodology integrates ball trajectory data, velocity measurements, and physics-based predictions to precisely quantify the discrepancy between theoretical and actual hittable positions. For training purposes, we developed an extensive dataset that meticulously documents the systematic variations between physics-model predictions and empirically observed real-world interception positions, enabling our system to learn these complex error patterns.

Specifically, we first compute the required joint angles using inverse kinematics (IK) to move the center of the paddle to the hittable position predicted by the physics-based model. Subsequently, a high-speed Spike camera [14] is employed to capture images of both the actual striking table tennis position and the paddle. Finally, the pixel distance between the ball's position and the paddle center in these images is used to estimate the true spatial deviation. Concurrently, we record the ball's position, velocity, and the hittable position predicted by the physics-based model.

The SONIC network processes three key inputs: position and velocity vectors from the preceding K frames, alongside the physics-based model's predicted hittable position. Each input stream—position vectors, velocity vectors, and estimated hittable positions—is independently processed through dedicated multi-layer perceptrons (MLPs). These MLPs incorporate ReLU activation functions and strategic dropout regularization to enhance generalization capabilities. The extracted features are subsequently concatenated into a comprehensive representation, which is then refined through a Transformer encoder architecture to capture sophisticated temporal dependencies within the trajectory data. Finally, an output module composed of fully connected layers generates the predicted deviation vector. Figure 2 provides a detailed visualization of the SONIC model architecture.

We optimize the model using the mean squared error (MSE) loss function, which minimizes the difference between the predicted and ground-truth deviation vectors.

$$L_{\text{MSE}}(\theta) = \frac{1}{N} \sum_{i=1}^N \|\hat{D}_i - D_i\|^2; \text{ where } \hat{D}_i = f_{\theta}([p_i, v_i, h_i]). \quad (3)$$

f_{θ} represents the neural network with parameters θ , $p_i \in \mathbb{R}^{K \times 3}$ denotes the position history, $v_i \in \mathbb{R}^{K \times 3}$ denotes the velocity history, $h_i \in \mathbb{R}^3$ denotes the expected hittable position, $D_i \in \mathbb{R}^2$ is the ground truth deviation vector, and $\hat{D}_i \in \mathbb{R}^2$ is the predicted deviation vector.

3.3 IMPACT: Imitation-based Motion Planning And Control Technology

After ensuring ball paddle interception through SONIC’s precise hittable position prediction, we propose **IMPACT** (Imitation-based Motion Planning And Control Technology) to derive the striking strategy for table tennis. This module learns strategic ball-hitting behaviors through imitation learning, enabling the robot to execute human-like tactical returns.

The IMPACT module requires accurate and diverse training samples that capture both the dynamic ball trajectories and ball landing region. Therefore, to collect such high-quality training data, we position the robotic arm at the hittable predicted by the SONIC using inverse kinematics (IK). Subsequently, based on the current state of the robotic arm moving to the hitting point, we add a randomly generated angle to three robot joints to execute the table tennis stroke. We record only those trials in which the ball is successfully returned on the opponent’s side of the table, and further classify them based on the specific landing region, enabling fine-grained control over hitting strategy.

The IMPACT module employs a transformer-based neural network that processes three types of input: ball trajectory data, robot joint configurations, and desired landing region signals (see Figure 2). Each modality is independently encoded into token representations using separate multi-layer perceptrons (MLPs). These tokens are then concatenated to form a unified input sequence, which is processed by a Transformer encoder to generate optimal adjustments for the joint angles.

To train the model, we employ the mean squared error (MSE) loss function, which minimizes the discrepancy between the predicted and ground-truth joint adjustments:

$$L_{MSE}(\theta') = \frac{1}{N} \sum_{i=1}^N \|\hat{J}_i - J_i\|^2; \text{ where } \hat{J}_i = f_{\theta'}([p_i, v_i, j_i, c_i]), j_i = \text{IK}(h_i). \quad (4)$$

$f_{\theta'}$ represents the transformer-based neural network with parameters θ' , $p_i \in \mathbb{R}^{K \times 3}$ denotes the position history, $v_i \in \mathbb{R}^{K \times 3}$ denotes the velocity history, $j_i \in \mathbb{R}^6$ represents the current 6-DOF robot joint configuration, $c_i \in \mathbb{R}^4$ represents the one-hot encoded control signal for the desired landing region, $J_i \in \mathbb{R}^3$ is the ground truth adjustment vector for the three critical joint angles, and $\hat{J}_i \in \mathbb{R}^3$ is the predicted joint adjustment vector.

Through this imitation-based approach, IMPACT enables the robot to adapt to different ball trajectories and target specific regions on the opponent’s court, transforming technical accuracy into tactical gameplay that significantly enhances the robot’s competitive capabilities in table tennis matches.

4 Experiments

In this section, we present comprehensive evaluations of SpikePingpong. In Section 4.1, we introduce our experimental setup, including dataset construction, implementation details, and evaluation metrics. Subsequently, we conduct extensive experiments to evaluate the ball-racket contact precision enabled by our SONIC module in Section 4.2. In Section 4.3, we assess the system’s spatial control capabilities for targeting across different table regions. Finally, we examine SpikePingpong’s ability to execute tactical sequences with consistent precision in Section 4.4, demonstrating the system’s reliability in complex gameplay scenarios.

4.1 Experiment Setting

Dataset. We introduce the SpikePingpong Dataset for our table tennis system, containing two distinct parts. The first part includes 0.5k samples collected using a high-speed spike camera operating at 20 kHz, with each sample containing trajectory information (position and velocity vectors from K=3 consecutive frames), expected hittable position, and ground truth deviation vectors. The second part consists of 2k successful return demonstrations, each containing ball trajectory information, predicted hittable position converted to joint configurations via inverse kinematics, and the joint adjustments that resulted in effective returns to specific court regions. All data was collected using an automated ball launching machine generating shots with randomized trajectories, spins, speeds, and angles within the robotic arm’s operational range, under controlled lighting conditions with a standardized racket. This comprehensive dataset provides the foundation for training both our trajectory prediction correction model and strategic return planning system.

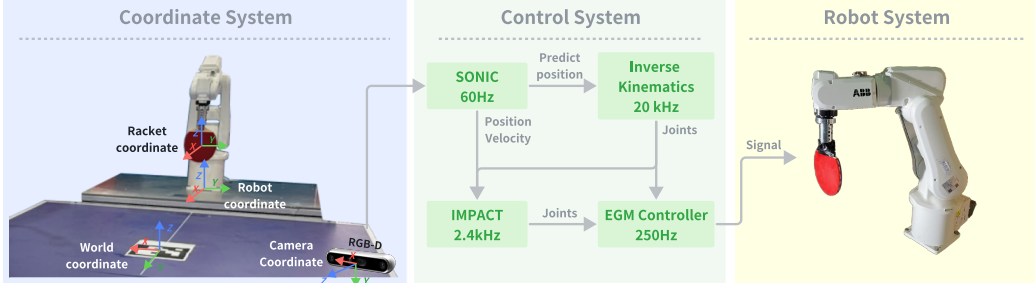


Figure 3: **System Overview.** Our system integrates three key subsystems: (1) a coordinate system for spatial tracking and transformation, (2) a multi-frequency control system with SONIC, IMPACT, and an EGM controller, and (3) a robot system based on the ABB IRB-120 arm equipped with a standard table tennis racket.

Implementation Details. As shown in Fig. 3, our system consists of three integrated subsystems. The coordinate system handles spatial transformations between world, camera, robot, and racket coordinates, with camera calibration performed before each session using ArUco markers to ensure accurate spatial measurements. The control system operates at multiple frequencies: the SONIC module processes ball trajectory data at 60Hz and predicts optimal interception positions, which are converted to joint configurations via inverse kinematics running at 20kHz. The IMPACT module operates at 2.4kHz to generate appropriate striking joint adjustments. These commands are transmitted to the EGM controller at 250Hz for responsive execution. The robot system employs an ABB IRB-120 robotic arm equipped with a standard table tennis racket, which receives and executes the control signals to perform the desired striking motions.

We implemented our comprehensive system on a workstation with an NVIDIA RTX 4090 GPU. For model training, the SONIC trajectory prediction module was trained for 2000 epochs using the Adam optimizer with a learning rate of 1e-3 and a cosine annealing learning rate schedule for optimal convergence. We used a batch size of 32, utilizing K=3 consecutive frames as input for robust trajectory prediction. The IMPACT strategic return module underwent similar rigorous training for 2000 epochs with identical optimization parameters but employed a reduced batch size of 4 to accommodate the complexity of the return planning task. All positional inputs were normalized to the range [0,1], while standard scaling was applied to velocity measurements to ensure numerical stability and consistent model performance across varying ball speeds and spin conditions.

Evaluation. To evaluate our system’s precision and accuracy, we adopt quantitative metrics based on spatial accuracy following established methodologies [13]. For ball-racket contact precision, we measure the mean absolute error (MAE) and root mean square error (RMSE) for contact deviation prediction, analyzing both overall accuracy and axis-specific performance (Y-axis horizontal and Z-axis vertical predictions). Visual evidence from spike camera captures provides additional validation of interception precision.

For landing accuracy, we divide the table tennis court into four specific regions, focusing on challenging aspects of ball placement control. We measure successful hit rate by calculating the percentage of balls landing within specified distances from the target position: primary accuracy zone (within 30cm of target center, 14% of reachable table area) and high precision zone (within 20cm of target center, 6% of reachable table area). This dual-threshold approach evaluates both general placement accuracy and high-precision targeting capabilities.

4.2 Ball-Racket Contact Precision Evaluation

Our SONIC module demonstrated significant improvements in predicting ball-racket contact deviations. Table 1 presents the quantitative results on the test set. The module achieved a mean absolute error (MAE) of 2.47mm and a

Table 1: Ball Hittable Position Prediction Error. Our SONIC module achieves millimeter-level accuracy across both axes, demonstrating superior precision in predicting the actual ball-racket contact point.

Metric	Value (mm)
Overall MAE	2.47
Overall RMSE	3.13
Y-axis MAE	2.98
Y-axis RMSE	3.69
Z-axis MAE	1.97
Z-axis RMSE	2.56

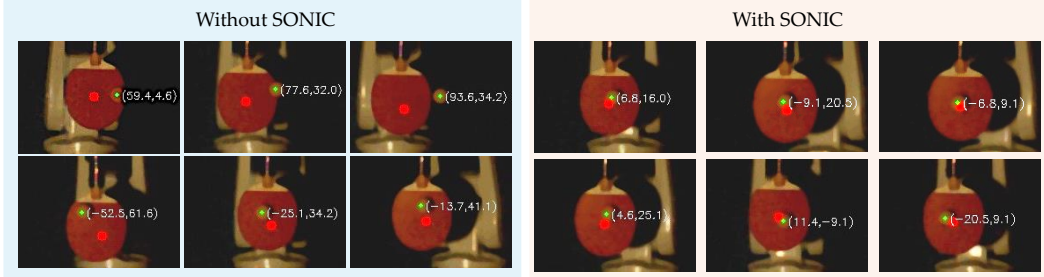


Figure 4: Visualization of ball-racket contact precision with and without SONIC. Spike-based camera images show the ball center (green) and racket center (red) at contact moment, with deviation measurements in millimeters. The reduced offset in the with-SONIC condition demonstrates the module’s effectiveness in achieving more precise ball interception.

root mean square error (RMSE) of 3.13mm for overall deviation prediction. Y-axis (horizontal) predictions showed superior accuracy with an MAE of 2.98mm, while Z-axis (vertical) predictions exhibited slightly lower error with an MAE of 1.97mm. As shown in Figure 4, SONIC substantially improves contact precision between ball and racket. The spike camera captures reveal a marked reduction in positional offsets when SONIC is activated, with minimal separation between ball center (green) and racket center (red), indicating highly accurate interception. This visual evidence corroborates the quantitative measurements and illustrates how SONIC’s millimeter-level prediction accuracy translates into improved physical contact precision.

4.3 Empirical Assessment of Spatial Control Capabilities

We conducted rigorous comparative evaluations against established baseline methods to comprehensively validate our system’s precision capabilities across four strategically positioned target regions (A, B, C, and D). Table 2 presents a comprehensive analysis of success rates across various target regions and precision thresholds. SpikePingpong exhibits exceptional performance, achieving an average success rate of 91% within the 30cm accuracy zone and 71% within the more challenging 20cm high-precision zone, substantially surpassing all comparative methods. Our system convincingly outperforms both human average capabilities and established approaches including LFP [29] and GoalsEye [13]. Common vision-language-action models like ACT [55] show significantly lower accuracy when trained on our dataset. Diffusion Policy [10] could not be evaluated due to its prohibitively high inference latency.

4.4 Sequential Target Execution Capabilities

To evaluate our system’s ability to execute tactical sequences, we designed a comprehensive experiment involving random target sequences spanning 20 consecutive returns (e.g., "BADCA..."). This challenging test rigorously assesses the system’s accuracy, reliability, and consistency throughout prolonged exchanges—a critical capability for realistic gameplay and competitive scenarios.

Table 3 presents the results of our multi-goal reaching experiment. SpikePingpong demonstrates exceptional performance, achieving an overall sequence success rate of $95\% \pm 5\%$ across these 20-shot sequences. This means that approximately 95% of individual shots within these sequences successfully reached their designated targets. The substantial performance enhancement provided by SONIC becomes clear when examining the ablation results, as removing this component reduces the

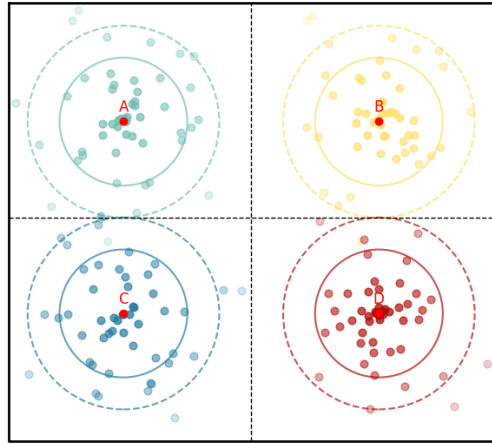


Figure 5: Spatial distribution of ball landing positions across four target regions. Each color represents a distinct target area, the concentric circles indicate the 20cm and 30cm precision thresholds.

Table 2: Single-Target Return Accuracy: Success rates for ball placement across four distinct target regions (A-D) at both 30cm and 20cm precision thresholds. The table compares human players, previous robotic approaches, and our SpikePingpong system, with and without the SONIC prediction module. Higher percentages indicate better performance, with values presented as mean \pm standard deviation where applicable.

Method	A		B		C		D		Avg.	
	30cm (%)	20cm (%)								
Human Avg.	26	8	30	10	32	18	30	16	30	13
LFP [29]	24	6	74	40	64	48	44	16	52	28
GoalsEye [13]	58	30	75	58	44	32	36	14	53	34
Diffusion Policy [10]	0	0	0	0	0	0	0	0	0	0
ACT [55]	11 \pm 4	4 \pm 2	12 \pm 5	4 \pm 1	10 \pm 3	2 \pm 1	14 \pm 4	5 \pm 2	12 \pm 4	4 \pm 2
SpikePingpong w/o SONIC	80 \pm 2	57 \pm 3	87 \pm 3	65 \pm 2	84 \pm 2	46 \pm 4	89 \pm 1	72 \pm 3	85 \pm 3	60 \pm 6
SpikePingpong	85 \pm 3(27 \uparrow)	65 \pm 7(35 \uparrow)	95 \pm 5(20 \uparrow)	71 \pm 5(13 \uparrow)	88 \pm 2(24 \uparrow)	66 \pm 2(18 \uparrow)	95 \pm 1(51 \uparrow)	83 \pm 3(67 \uparrow)	91 \pm 5(38 \uparrow)	71 \pm 7(37 \uparrow)

Table 3: Sequential Target Execution Performance: Success rates for 20-shot random target sequences. The Success Rate column shows the percentage of individual shots successfully reaching their designated targets within sequences, while subsequent columns present region-specific success rates at both 30cm and 20cm precision thresholds.

Method	Success Rate(%)	A		B		C		D	
		30cm (%)	20cm (%)	30cm (%)	20cm (%)	30cm (%)	20cm (%)	30cm (%)	20cm (%)
Diffusion Policy [55]	0	0	0	0	0	0	0	0	0
ACT [55]	11 \pm 3	7	2	11	5	9	5	14	6
SpikePingpong w/o SONIC	88 \pm 4	80	65	92	58	76	65	90	78
SpikePingpong	95 \pm 5(84 \uparrow)	92(85 \uparrow)	77(75 \uparrow)	100(89 \uparrow)	66(61 \uparrow)	88(79 \uparrow)	83(78 \uparrow)	100(86 \uparrow)	81(75 \uparrow)

success rate to 88% \pm 4%. These results demonstrate that our system not only excels at individual shot placement but can maintain precision while executing complex, extended tactical sequences. This capability represents a significant advancement toward robot table tennis systems that can implement sustained strategic gameplay rather than merely returning balls, suggesting potential for developing higher-level strategic planning modules.

4.5 Computational Efficiency

Real-time responsiveness is paramount in table tennis robotics. As demonstrated in Table 4, our approach exhibits remarkable computational efficiency. SpikePingpong achieves an inference latency of merely 0.407ms, dramatically outpacing Diffusion Policy and substantially exceeding ACT’s performance. Our system’s rapid inference capability provides adequate time for physical actuation after decision-making, supporting responsive gameplay in real-world conditions.

5 Conclusions

In this paper, we presented SpikePingpong, a high-precision robotic table tennis system integrating spike-based vision and advanced control techniques. Our system combines SONIC, achieving millimeter-level ball-racket contact precision, and IMPACT, enabling accurate ball striking to specified target regions.. Experiments demonstrate superior performance with 91% success in the primary accuracy zone and 71% in the high-precision zone, significantly outperforming previous systems. With an inference time of just 0.407ms, SpikePingpong enables real-time decision-making while executing extended tactical sequences with a 95% completion rate. Despite these achievements, our system has limitations: it does not account for ball spin, which affects optimal interception strategies for different spin types. Additionally, performance against human players remains challenging due to the complex and unpredictable trajectories humans generate compared to our training conditions. Future work will focus on incorporating spin modeling, enhancing adaptability to diverse playing styles, and developing strategic gameplay planning for human-robot interaction. SpikePingpong advances robotic control for fast-paced tasks requiring precise spatiotemporal coordination.

Table 4: Computational Performance Comparison: Average inference times in milliseconds for generating return actions across different methods.

Method	Inference time (ms)
Diffusion Policy [10]	2437.22
ACT [55]	7.15
SpikePingpong	0.407

References

- [1] Saminda Wishwajith Abeyruwan, Laura Graesser, David B D'Ambrosio, Avi Singh, Anish Shankar, Alex Bewley, Deepali Jain, Krzysztof Marcin Choromanski, and Pannag R Sanketi. i-sim2real: Reinforcement learning of robotic policies in tight human-robot interaction loops. In *Conference on Robot Learning*, pages 212–224. PMLR, 2023.
- [2] Leopoldo Acosta, JJ Rodrigo, Juan A Mendez, G Nicolás Marichal, and Marta Sigut. Ping-pong player prototype. *IEEE robotics & automation magazine*, 10(4):44–52, 2003.
- [3] Sonya Alexandrova, Zachary Tatlock, and Maya Cakmak. Roboflow: A flow-based visual programming language for mobile manipulation tasks. In *2015 IEEE international conference on robotics and automation (ICRA)*, pages 5537–5544. IEEE, 2015.
- [4] Luca Anzalone, Paola Barra, Silvio Barra, Aniello Castiglione, and Michele Nappi. An end-to-end curriculum learning approach for autonomous driving scenarios. *IEEE Transactions on Intelligent Transportation Systems*, 23(10):19817–19826, 2022.
- [5] Yahav Avigal, Lars Berscheid, Tamim Asfour, Torsten Kröger, and Ken Goldberg. Speedfolding: Learning efficient bimanual folding of garments. In *2022 IEEE/RSJ International Conference on Intelligent Robots and Systems (IROS)*, pages 1–8. IEEE, 2022.
- [6] Qingwei Ben, Feiyu Jia, Jia Zeng, Junting Dong, Dahua Lin, and Jiangmiao Pang. Homie: Humanoid loco-manipulation with isomorphic exoskeleton cockpit. *arXiv preprint arXiv:2502.13013*, 2025.
- [7] J. Billingsley. Robot ping pong. *Practical Computing*, 1983.
- [8] bubbliliing. yolov4-tiny-pytorch: PyTorch implementation of YOLOv4-tiny. <https://github.com/bubbliliing/yolov4-tiny-pytorch>, 2020.
- [9] Dieter Büchler, Simon Guist, Roberto Calandra, Vincent Berenz, Bernhard Schölkopf, and Jan Peters. Learning to play table tennis from scratch using muscular robots. *CoRR*, abs/2006.05935, 2020.
- [10] Cheng Chi, Zhenjia Xu, Siyuan Feng, Eric Cousineau, Yilun Du, Benjamin Burchfiel, Russ Tedrake, and Shuran Song. Diffusion policy: Visuomotor policy learning via action diffusion. *The International Journal of Robotics Research*, page 02783649241273668, 2023.
- [11] David B D'Ambrosio, Jonathan Abelian, Saminda Abeyruwan, Michael Ahn, Alex Bewley, Justin Boyd, Krzysztof Choromanski, Omar Cortes, Erwin Coumans, Tianli Ding, et al. Robotic table tennis: A case study into a high speed learning system. *arXiv preprint arXiv:2309.03315*, 2023.
- [12] desigproject. tt2 dataset. <https://universe.roboflow.com/desigproject/tt2-cyt9i>, dec 2022. visited on 2025-05-12.
- [13] Tianli Ding, Laura Graesser, Saminda Abeyruwan, David B D'Ambrosio, Anish Shankar, Pierre Serenanet, Pannag R Sanketi, and Corey Lynch. Goalseye: Learning high speed precision table tennis on a physical robot. *arXiv preprint arXiv:2210.03662*, 2022.
- [14] Siwei Dong, Tiejun Huang, and Yonghong Tian. Spike camera and its coding methods. *arXiv preprint arXiv:2104.04669*, 2021.
- [15] Yankai Fu, Qiuxuan Feng, Ning Chen, Zichen Zhou, Mengzhen Liu, Mingdong Wu, Tianxing Chen, Shanyu Rong, Jiaming Liu, Hao Dong, et al. Cordvip: Correspondence-based visuomotor policy for dexterous manipulation in real-world. *arXiv preprint arXiv:2502.08449*, 2025.
- [16] Wenbo Gao, Laura Graesser, Krzysztof Choromanski, Xingyou Song, Nevena Lazic, Pannag Sanketi, Vikas Sindhwani, and Navdeep Jaitly. Robotic table tennis with model-free reinforcement learning. In *IROS*, 2020.
- [17] Xiaoshan Gao, Liang Yan, Zhijun Li, Gang Wang, and I-Ming Chen. Improved deep deterministic policy gradient for dynamic obstacle avoidance of mobile robot. *IEEE Transactions on Systems, Man, and Cybernetics: Systems*, 53(6):3675–3682, 2023.

[18] Tuomas Haarnoja, Sehoon Ha, Aurick Zhou, Jie Tan, George Tucker, and Sergey Levine. Learning to walk via deep reinforcement learning. *arXiv preprint arXiv:1812.11103*, 2018.

[19] Tairan He, Jiawei Gao, Wenli Xiao, Yuanhang Zhang, Zi Wang, Jiashun Wang, Zhengyi Luo, Guanqi He, Nikhil Sobanbabu, Chaoyi Pan, Zeji Yi, Guannan Qu, Kris Kitani, Jessica Hodgins, Linxi "Jim" Fan, Yuke Zhu, Changliu Liu, and Guanya Shi. Asap: Aligning simulation and real-world physics for learning agile humanoid whole-body skills. *arXiv preprint arXiv:2502.01143*, 2025.

[20] Tairan He, Zhengyi Luo, Xialin He, Wenli Xiao, Chong Zhang, Weinan Zhang, Kris Kitani, Changliu Liu, and Guanya Shi. Omnih2o: Universal and dexterous human-to-humanoid whole-body teleoperation and learning. *arXiv preprint arXiv:2406.08858*, 2024.

[21] Zhe Hu, Yu Zheng, and Jia Pan. Grasping living objects with adversarial behaviors using inverse reinforcement learning. *IEEE Transactions on Robotics*, 39(2):1151–1163, 2023.

[22] Binghao Huang, Yuanpei Chen, Tianyu Wang, Yuzhe Qin, Yaodong Yang, Nikolay Atanasov, and Xiaolong Wang. Dynamic handover: Throw and catch with bimanual hands. *arXiv preprint arXiv:2309.05655*, 2023.

[23] Yanlong Huang, Dieter Buchler, Okan Koç, Bernhard Schölkopf, and Jan Peters. Jointly learning trajectory generation and hitting point prediction in robot table tennis. In *IEEE-RAS International Conference on Humanoid Robots (Humanoids)*, 2016.

[24] Seungsu Kim, Ashwini Shukla, and Aude Billard. Catching objects in flight. *IEEE Transactions on Robotics*, 30(5):1049–1065, 2014.

[25] Jens Kober, Erhan Öztop, and Jan Peters. Reinforcement learning to adjust robot movements to new situations. In *IJCAI Proceedings-International Joint Conference on Artificial Intelligence*, volume 22, page 2650. Citeseer, 2011.

[26] Okan Koç, Guilherme Maeda, and Jan Peters. Online optimal trajectory generation for robot table tennis. *Robotics and Autonomous Systems*, 2018.

[27] Fengbo Lan, Shengjie Wang, Yunzhe Zhang, Haotian Xu, Oluwatosin Oseni, Ziye Zhang, Yang Gao, and Tao Zhang. Dexcatch: Learning to catch arbitrary objects with dexterous hands. *arXiv preprint arXiv:2310.08809*, 2023.

[28] Xinyuan Luo, Shengmiao Jin, Hung-Jui Huang, and Wenzhen Yuan. An intelligent robotic system for perceptive pancake batter stirring and precise pouring. In *2024 IEEE/RSJ International Conference on Intelligent Robots and Systems (IROS)*, pages 5970–5977. IEEE, 2024.

[29] Corey Lynch, Mohi Khansari, Ted Xiao, Vikash Kumar, Jonathan Tompson, Sergey Levine, and Pierre Sermanet. Learning latent plans from play. In *Conference on robot learning*, pages 1113–1132. Pmlr, 2020.

[30] Michiya Matsushima, Takaaki Hashimoto, and Fumio Miyazaki. Learning to the robot table tennis task: ball control and rally with a human. In *IEEE International Conference on Systems, Man and Cybernetics*, 2003.

[31] Fumio Miyazaki, Masahiro Takeuchi, Michiya Matsushima, Takamichi Kusano, and Takaaki Hashimoto. Realization of the table tennis task based on virtual targets. In *Proceedings of the IEEE International Conference on Robotics and Automation (ICRA)*, 2002.

[32] Shotaro Mori, Kazutoshi Tanaka, Satoshi Nishikawa, Ryuma Niiyama, and Yasuo Kuniyoshi. High-speed humanoid robot arm for badminton using pneumatic-electric hybrid actuators. *IEEE Robotics and Automation Letters*, 4(4):3601–3608, 2019.

[33] Urs Muller, Jan Ben, Eric Cosatto, Beat Flepp, and Yann Cun. Off-road obstacle avoidance through end-to-end learning. *Advances in neural information processing systems*, 18, 2005.

[34] Katharina Mülling, Jens Kober, Oliver Kroemer, and Jan Peters. Learning to select and generalize striking movements in robot table tennis. *The International Journal of Robotics Research*, 32(3):263–279, 2013.

[35] Katharina Mülling, Jens Kober, and Jan Peters. A biomimetic approach to robot table tennis. In *2010 IEEE/RSJ International Conference on Intelligent Robots and Systems*, pages 1921–1926. IEEE, 2010.

[36] Ramkumar Natarajan, Hanlan Yang, Qintong Xie, Yash Oza, Manash Pratim Das, Fahad Islam, Muhammad Suhail Saleem, Howie Choset, and Maxim Likhachev. Preprocessing-based kinodynamic motion planning framework for intercepting projectiles using a robot manipulator. In *2024 IEEE International Conference on Robotics and Automation (ICRA)*, pages 10910–10916. IEEE, 2024.

[37] Quan Nguyen, Ayush Agrawal, Xingye Da, William C Martin, Hartmut Geyer, Jessy W Grizzle, and Koushil Sreenath. Dynamic walking on randomly-varying discrete terrain with one-step preview. In *Robotics: Science and Systems*, volume 2, pages 384–99, 2017.

[38] Yunpeng Pan, Ching-An Cheng, Kamil Saigol, Keuntaek Lee, Xinyan Yan, Evangelos Theodorou, and Byron Boots. Agile autonomous driving using end-to-end deep imitation learning. *arXiv preprint arXiv:1709.07174*, 2017.

[39] Yunpeng Pan, Ching-An Cheng, Kamil Saigol, Keuntaek Lee, Xinyan Yan, Evangelos A Theodorou, and Byron Boots. Imitation learning for agile autonomous driving. *The International Journal of Robotics Research*, 39(2-3):286–302, 2020.

[40] pingpong. Ping pong detection dataset. <https://universe.roboflow.com/pingpong-ojuhj/ping-pong-detection-0guzq>, may 2024. visited on 2025-05-12.

[41] Dean A Pomerleau. Alvinn: An autonomous land vehicle in a neural network. *Advances in neural information processing systems*, 1, 1988.

[42] Lin Shao, Fabio Ferreira, Mikael Jorda, Varun Nambiar, Jianlan Luo, Eugen Solowjow, Juan Aparicio Ojea, Oussama Khatib, and Jeannette Bohg. Unigrasp: Learning a unified model to grasp with multifingered robotic hands. *IEEE Robotics and Automation Letters*, 5(2):2286–2293, 2020.

[43] Luis Angel Silva, José María Sebastián, R Saltaren, Rafael Aracil, and Jose Sanpedro. Robotenis: optimal design of a parallel robot with high performance. In *2005 IEEE/RSJ International Conference on Intelligent Robots and Systems*, pages 2134–2139. IEEE, 2005.

[44] Jie Tan, Tingnan Zhang, Erwin Coumans, Atil Iscen, Yunfei Bai, Danijar Hafner, Steven Bohez, and Vincent Vanhoucke. Sim-to-real: Learning agile locomotion for quadruped robots. *arXiv preprint arXiv:1804.10332*, 2018.

[45] Jonas Tebbe, Lukas Krauch, Yapeng Gao, and Andreas Zell. Sample-efficient reinforcement learning in robotic table tennis. In *ICRA*, 2021.

[46] An Dinh Vuong, Minh Nhat Vu, Hieu Le, Baoru Huang, Huynh Thi Thanh Binh, Thieu Vo, Andreas Kugi, and Anh Nguyen. Grasp-anything: Large-scale grasp dataset from foundation models. In *2024 IEEE International Conference on Robotics and Automation (ICRA)*, pages 14030–14037. IEEE, 2024.

[47] Yilei Wang and Ling Wang. [retracted] machine vision-based ping pong ball rotation trajectory tracking algorithm. *Computational Intelligence and Neuroscience*, 2022(1):3835649, 2022.

[48] Zhongli Wang, Guohui Tian, and Shijie Guo. Gmm enabled by multimodal information fusion network for detection and motion planning of robotic liquid pouring. *IEEE Transactions on Neural Networks and Learning Systems*, 2024.

[49] Ruihai Wu, Haoran Lu, Yiyan Wang, Yubo Wang, and Hao Dong. Unigarmentmanip: A unified framework for category-level garment manipulation via dense visual correspondence. In *Proceedings of the IEEE/CVF Conference on Computer Vision and Pattern Recognition*, pages 16340–16350, 2024.

[50] Ping Yang, De Xu, Huawei Wang, and Zhengtao Zhang. Control system design for a 5-dof table tennis robot. In *2010 11th International Conference on Control Automation Robotics & Vision*, pages 1731–1735. IEEE, 2010.

- [51] Andy Zeng, Shuran Song, Johnny Lee, Alberto Rodriguez, and Thomas Funkhouser. Tossingbot: Learning to throw arbitrary objects with residual physics. *IEEE Transactions on Robotics*, 36(4):1307–1319, 2020.
- [52] Chong Zhang, Wenli Xiao, Tairan He, and Guanya Shi. Wococo: Learning whole-body humanoid control with sequential contacts. *arXiv e-prints*, pages arXiv–2406, 2024.
- [53] Kun Zhang, Zhiqiang Cao, Jianran Liu, Zaojun Fang, and Min Tan. Real-time visual measurement with opponent hitting behavior for table tennis robot. *IEEE Transactions on Instrumentation and Measurement*, 67(4):811–820, 2018.
- [54] Yuanhang Zhang, Tianhai Liang, Zhenyang Chen, Yanjie Ze, and Huazhe Xu. Catch it! learning to catch in flight with mobile dexterous hands. *arXiv preprint arXiv:2409.10319*, 2024.
- [55] Tony Z Zhao, Vikash Kumar, Sergey Levine, and Chelsea Finn. Learning fine-grained bimanual manipulation with low-cost hardware. *arXiv preprint arXiv:2304.13705*, 2023.
- [56] Zida Zhao, Haodong Huang, Shilong Sun, Jing Jin, and Wenjie Lu. Reinforcement learning for dynamic task execution: A robotic arm for playing table tennis. In *2024 IEEE International Conference on Robotics and Biomimetics (ROBIO)*, pages 608–613. IEEE, 2024.
- [57] Yichao Zhong, Chong Zhang, Tairan He, and Guanya Shi. Bridging adaptivity and safety: Learning agile collision-free locomotion across varied physics. *arXiv preprint arXiv:2501.04276*, 2025.

A Overview

Due to space limitations, we provide additional details of the proposed method in this supplementary material. In Appendix B, we present a comprehensive overview of our system architecture, including the ball launching mechanism, multi-camera vision setup, and robotic execution components. Appendix C elaborates on our ball detection and trajectory prediction methods, featuring our YOLOv4-tiny implementation, motion state estimation filtering, and hittable position prediction algorithms. In Appendix D, we describe our two specialized datasets: one for the SONIC model focusing on precise paddle-ball contact control, and another for the IMPACT model targeting effective hitting strategies. Finally, Appendix E summarizes our real-world experiments, demonstrating the system’s ability to return balls to specific target locations with high precision when tested with a ball machine, as well as video recordings of human-robot gameplay.

B System Overview

Our system consists of a ball launcher, high-speed camera, depth camera, RGB camera, and robotic arm, designed to achieve an automated table tennis playing system.

B.1 Ball Launching System

We employ the intelligent table tennis robot PONGBOT NOVA as our ball launching system. This table-mounted launcher can generate topspin and backspin, with precise landing point control ranging from -2 to +2, and adjustable ball speed between levels 1-3, providing stable and controllable ball trajectories for our experiments.

B.2 Vision System

The vision system comprises three cameras, each dedicated to different tasks:

- **High-Speed Camera:** Spike M1K40-H2-Gen3 with a resolution of 1000×1000 and a maximum frame rate of 20,000 fps. In our experiments, we set a step size of 200, saving 100 images per second, specifically designed to capture the instantaneous contact between the ball and the paddle, providing high temporal resolution image data for stroke analysis.
- **Depth Camera:** Intel RealSense D455 with a resolution of 640×480 and a frame rate of 60Hz. This camera is calibrated using ArUco markers and employs YOLO [8] model for ball detection. The system transforms detected pixel coordinates into world coordinates through intrinsic and extrinsic parameters, enabling real-time tracking of the ball’s position.
- **RGB Camera:** Intel RealSense LiDAR Camera L515 with a resolution of 960×540 and a frame rate of 60Hz. It primarily detects the landing position of the ball after being hit by the robot, providing feedback for evaluating stroke effectiveness.

B.3 Mechanical Execution System

The execution system utilizes an ABB IRB 120 6 DoF (six-degree-of-freedom) robotic arm with maximum joint rotation speeds of $250^\circ/\text{s}$, $250^\circ/\text{s}$, $250^\circ/\text{s}$, $320^\circ/\text{s}$, $320^\circ/\text{s}$, and $420^\circ/\text{s}$, respectively. The arm is equipped with a standard table tennis paddle at its end-effector to execute the optimal hitting motion calculated by the system.

This system achieves real-time tracking and precise hitting of table tennis balls through the tight integration of visual perception, trajectory prediction, and motion planning, providing a comprehensive experimental platform for table tennis robotics research.

C Details of Ball Detection and Trajectory Prediction

C.1 Ball Detection

In the context of high-speed robotic table tennis, where accurate timing and spatial awareness are critical, a high-frequency vision system is required to continuously track the ball’s position for

real-time trajectory estimation and manipulation control. Thus, we chose YOLOv4-tiny [8] due to its lightweight design and computational efficiency, enabling a detection frequency of up to **150 Hz**, which is crucial for the precise and timely interaction with the fast-moving ball. The initial phase of our research involves the supervised training of the detection model using publicly available datasets: Roboflow [3], TT2 [12], and Ping Pong Detection [40]. A two-phase training strategy is implemented to enhance model robustness. In the first phase, the model is trained on the complete dataset. In the second phase, samples that were misdetected during the initial training are selectively sampled and assigned higher weights for fine-tuning, with the goal of improving the detector’s accuracy on difficult instances. Our empirical validation is conducted using an Intel RealSense D455 RGB-D camera, where we employ the optimized lightweight detection model. This setup achieves a detection accuracy that exceeds 99.8%, facilitating rapid and precise 2D positional detection. The visualization results are shown in Figure 6.

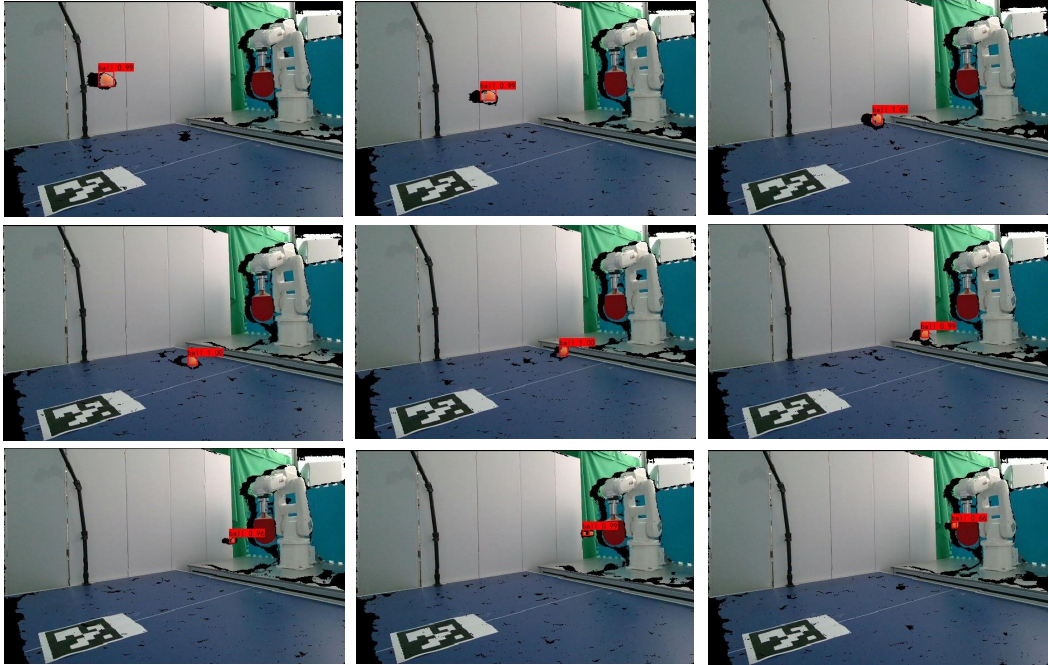


Figure 6: **Visualization of ball detection.** The sequence shows the ball’s trajectory at different time points with accurately placed bounding boxes around the detected ball. Our YOLOv4-tiny model consistently identifies the ball’s position even during high-speed motion, demonstrating the robustness of our detection approach under various lighting conditions and ball velocities.

C.2 Motion State Estimation Filter

To accurately track the ball’s motion state, we designed a filtering algorithm that combines physical models with measurement data. This algorithm not only smooths noise in the ball position data but also provides accurate velocity estimates, establishing a foundation for subsequent trajectory prediction and interception planning.

Exponential Moving Average Filter We implemented a physics-based Exponential Moving Average (EMA) filter that simultaneously estimates both position and velocity by combining system dynamics models with real-time observation data. The core formula of the filter is:

$$\hat{x}_t = (1 - \alpha) \cdot f(\hat{x}_{t-1}) + \alpha \cdot z_t \quad (5)$$

where \hat{x}_t is the current state estimate, $f(\hat{x}_{t-1})$ is the dynamics prediction based on the previous state estimate, z_t is the current observation, α is the mixing constant that determines the weight ratio between observation and prediction.

For the ball's free-fall motion, we adopted standard ballistic equations as the dynamics model. Specifically, the prediction equations for position and velocity are:

$$\hat{p}_t = \hat{p}_{t-1} + \hat{v}_{t-1} \cdot \Delta t + \frac{1}{2} a \cdot \Delta t^2, \quad (6)$$

$$\hat{v}_t = \hat{v}_{t-1} + a \cdot \Delta t. \quad (7)$$

where, \hat{p}_t is the position estimate, \hat{v}_t is the velocity estimate, Δt is the time step, a is the acceleration (gravity acceleration -9.81 m/s^2 in the z-direction, 0 in x and y directions).

Considering the different motion characteristics of the ball in different directions, we applied different mixing constants for the x, y, and z directions: $\alpha_x = 0.15$, $\alpha_y = 0.15$, $\alpha_z = 0.25$. The larger mixing constant for the z-direction was chosen to better adapt to the faster velocity changes in the vertical direction due to gravity. Additionally, we implemented special handling for the ascending phase in the z-direction to more accurately capture the motion characteristics of the initial segment of the parabolic trajectory.

Implementation Details The system maintains a fixed-length (3 frames) history data queue for calculating initial velocity and handling data interruptions. When a data stream interruption exceeding 1 second is detected, the filter automatically resets the historical data to avoid the influence of outdated information on current estimates. This adaptive mechanism enables the system to quickly resume normal operation when the ball reappears or a new throw begins.

Performance Visualization Experiments show that this filter effectively smooths noise in the raw position data while providing accurate velocity estimates. Since the ball detection algorithm already provides relatively accurate position information, the filter primarily serves to refine and stabilize estimates, particularly excelling in velocity calculation. The filtered trajectory data exhibits smooth parabolic characteristics consistent with physical laws, providing a reliable foundation for subsequent trajectory prediction as shown in Figure 7.

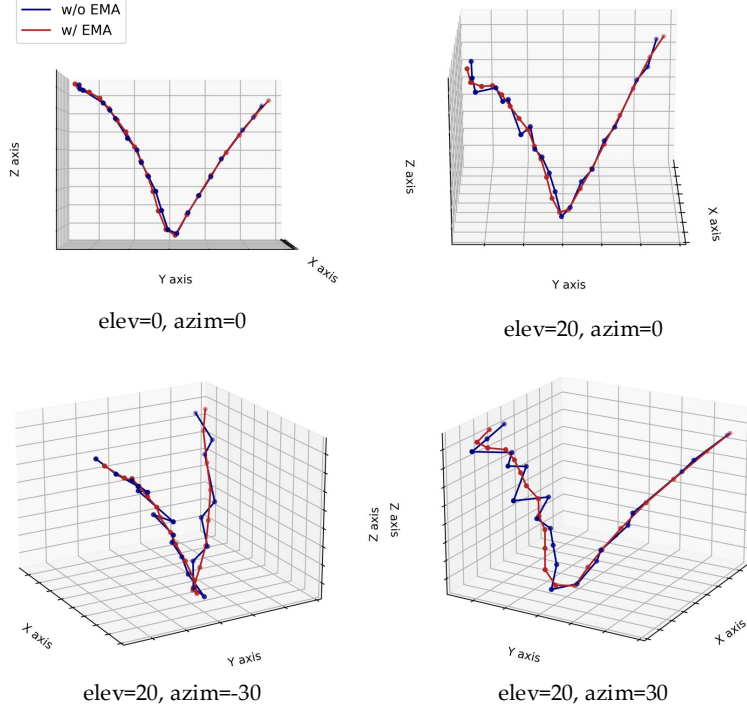


Figure 7: **Comparison of ball trajectory with and without EMA filtering.** The figure displays trajectories from multiple viewing angles, with red curves showing raw detection data and blue curves showing EMA-filtered results. The filtering effectively removes noise while maintaining the ball's natural parabolic motion, providing more reliable data for trajectory prediction.

C.3 Hittable Position Prediction

To enable the robot to intercept the ball effectively, we developed a trajectory prediction algorithm that estimates where and when the ball will reach a hittable position. This algorithm leverages the filtered position and velocity data from our EMA filter to project the ball’s future path.

Ballistic Model Implementation Our prediction algorithm employs a simplified ballistic model that accounts for gravitational acceleration (9.81 m/s^2), initial position and velocity vectors, and coefficient of restitution for potential bounces. The model deliberately excludes spin effects and complex aerodynamics to maintain computational efficiency and implementation simplicity across both simulation and real-world environments.

Trajectory Prediction The prediction process is implemented using the following Algorithm 1. This algorithm applies the ballistic equations to project the ball’s trajectory forward in time and determine exactly when and where it will intersect the hitting plane. The computed hittable position, impact velocity, and arrival time are then passed to the robot control system for interception planning.

Algorithm 1 Predict Hittable Position

Require: p_0 (initial position), v_0 (initial velocity), $t_{current}$ (current time), y_{plane} (hitting plane y-coordinate)

Ensure: Returns hit position, velocity and arrival time, or null if not hittable

- 1: $g \leftarrow (0, 0, -9.81)$ Gravity vector
- 2: **if** $|v_0.y| < \epsilon$ **then**
- 3: Ball moving parallel to hitting plane
- 4: **return** null
- 5: **end if**
- 6: $t_{hit} \leftarrow (y_{plane} - p_0.y) / v_0.y$
- 7: **if** $t_{hit} < 0$ **then**
- 8: Ball already passed the plane
- 9: **return** null
- 10: **end if**
- 11: $p_{hit} \leftarrow p_0 + v_0 \cdot t_{hit} + \frac{1}{2}g \cdot t_{hit}^2$
- 12: $p_{hit}.y \leftarrow y_{plane}$ Ensure exact y-coordinate
- 13: $v_{hit} \leftarrow v_0 + g \cdot t_{hit}$
- 14: $t_{arrival} \leftarrow t_{current} + t_{hit}$
- 15: **return** $(p_{hit}, v_{hit}, t_{arrival})$

The prediction algorithm includes special handling for various scenarios: trajectories that never intersect the hitting plane, balls moving away from the hitting plane, multiple potential intersections (selecting the earliest valid one), and bounces off other surfaces before reaching the hitting plane.

Integration with Robot Control The predicted hittable position, impact velocity, and arrival time are continuously updated and provided to the robot control system, enabling it to plan and execute appropriate interception movements. This real-time prediction allows the robot to adjust its position and orientation to successfully hit the ball even when the ball follows an unexpected trajectory.

D Dataset Description

This section details the two critical datasets developed for our table tennis robot system. These datasets support the system’s two core components: the SONIC model (Spike-Oriented Neural Improvement Calibrator) focused on precise paddle-contact control and the IMPACT model (Imitation-based Motion Planning And Control Technology) focused on effective hitting strategies. Below, we describe the collection processes, annotation methods, and how these datasets provide the foundation for the system’s performance.

D.1 Dataset for SONIC

D.1.1 Data Collection Process

Our data collection process involves the following steps: The ball launcher randomly serves balls within a predetermined range. Based on the Ball Detection and Trajectory Prediction framework described above, we use the Intel RealSense D455 camera to record trajectory information, including position and velocity vectors. Once a hittable position is predicted, this coordinate is transformed into the robotic arm’s base coordinate system. Using PyBullet, we compute the inverse kinematics to determine the joint values required to move to this position, which are then sent to the robotic arm via an EGM Controller. Leveraging the high frame rate capability of the Spike camera, we capture images of the exact moment of contact between the ball and the paddle. This process is repeated multiple times to build a comprehensive dataset.

D.1.2 Data Annotation Process

Pixel-to-Real-World Conversion A critical step in our data annotation process was establishing an accurate conversion ratio between pixel measurements in images and real-world dimensions. We developed a systematic approach using the known dimensions of the table tennis paddle as a reference.

The process involves the following steps:

1. **Image Acquisition:** We captured multiple high-resolution images of the table tennis paddle using the Spike camera.
2. **Image Preprocessing:** Each image undergoes preprocessing to reduce noise and enhance contrast, facilitating more accurate edge detection. We apply a center-crop operation to focus on the region containing the paddle.
3. **Paddle Detection:** Using color-based segmentation, we isolate the paddle from the background by defining a target color range (RGB: 65, 31, 31) with an appropriate tolerance value. This creates a binary mask representing the paddle area.
4. **Morphological Operations:** To refine the mask, we apply morphological operations including opening (to remove small noise artifacts) and closing (to fill small holes), using a 5×5 kernel.
5. **Connected Component Analysis:** We identify the largest connected component in the mask, which corresponds to the paddle, and filter out smaller noise components.
6. **Minimum Area Rectangle Fitting:** For the detected paddle region, we compute the minimum area rectangle that encloses the paddle contour, providing us with the paddle’s pixel dimensions (width and height).
7. **Conversion Ratio Calculation:** Knowing the actual paddle dimensions (150mm \times 150mm), we calculate the conversion ratio for both width and height:

$$\text{mm_per_pixel_width} = \frac{\text{real_width_mm}}{\text{width_pixels}} \quad (8)$$

$$\text{mm_per_pixel_height} = \frac{\text{real_height_mm}}{\text{height_pixels}} \quad (9)$$

8. **Average Conversion Ratio:** To improve accuracy, we average the width and height conversion ratios:

$$\text{mm_per_pixel_avg} = \frac{\text{mm_per_pixel_width} + \text{mm_per_pixel_height}}{2} \quad (10)$$

9. **Multiple Image Processing:** We repeat this process across multiple images and compute the overall average conversion ratio to minimize measurement errors.

This methodology yielded a reliable pixel-to-millimeter conversion factor that was subsequently used throughout our data annotation pipeline to transform pixel coordinates in images to real-world spatial coordinates.

D.1.3 Ball-Paddle Contact Detection

After establishing the pixel-to-millimeter conversion ratio, we developed a comprehensive algorithm to detect and analyze the contact between the table tennis ball and paddle in high-speed scenarios. This process is particularly challenging due to the rapid nature of the contact event, which typically occurs within milliseconds.

Our detection pipeline consists of the following key components:

1. **High Temporal Resolution Acquisition:** The Spike camera captures the ball-paddle interaction with exceptional temporal precision (microsecond-level), providing detailed information about the contact dynamics that conventional cameras would miss. The neuromorphic vision sensor outputs asynchronous spike signals rather than traditional frame-based images, enabling ultra-high temporal resolution.
2. **Ball Detection Strategy:** We implemented a dual-approach ball detection method:
 - **Hole-based Detection:** The primary method identifies the ball as a hole or void within the paddle region during contact. This approach is particularly effective when the ball partially occludes the paddle.
 - **Color-based Detection:** As a complementary approach, we detect the ball using a predefined color range (RGB: 79, 58, 34) with appropriate tolerance values, creating a binary mask for potential ball regions.
3. **Circularity Filtering:** To distinguish the ball from other objects or noise, we apply a circularity measure to each detected region:

$$\text{Circularity} = \frac{4\pi \times \text{Area}}{\text{Perimeter}^2} \quad (11)$$

Regions with circularity above 0.6 are considered potential ball candidates, as table tennis balls maintain their circular appearance even during high-speed motion.

4. **Proximity Analysis:** We prioritize detected ball regions that are within a 20-pixel radius of the paddle's edge, as these are most likely to represent actual contact points.
5. **Temporal Sequence Analysis:** By analyzing the sequential spike signals from the neuromorphic camera, we track the ball's trajectory before, during, and after contact with the paddle. This allows us to determine the exact moment of impact with microsecond precision.
6. **Coordinate System Transformation:** After detecting both the paddle and ball, we establish a paddle-centered coordinate system:
 - **Origin:** Center of the paddle
 - **X-axis:** Horizontal direction (positive rightward)
 - **Y-axis:** Vertical direction (positive upward)
7. **Contact Point Calculation:** The ball's position is transformed from pixel coordinates to this paddle-centered coordinate system and then converted to physical units (millimeters) using our established conversion ratio:

$$x_{\text{mm}} = (x_{\text{ball}} - x_{\text{paddle}}) \times \text{mm_per_pixel} \quad (12)$$

$$y_{\text{mm}} = (y_{\text{paddle}} - y_{\text{ball}}) \times \text{mm_per_pixel} \quad (13)$$

This ball-paddle contact detection methodology provides unprecedented insights into the dynamics of table tennis interactions. By leveraging the unique capabilities of neuromorphic vision sensors, we can capture and analyze high-speed interactions that would be impossible to observe with conventional imaging systems. The resulting data enables quantitative analysis of contact timing, location, and dynamics, which can be valuable for both sports science research and athlete training applications.

D.2 Dataset for IMPACT

D.2.1 Data Collection Process

After successfully training the SONIC model to ensure precise ball-paddle contact near the center of the paddle, we extended our data collection to include the hitting phase. Building upon our established

interception capabilities, we implemented a structured process to collect data on effective hitting techniques. For the hitting phase data collection, we augmented our previous methodology with the following approach:

1. **Randomized Joint Angle Sampling:** To generate diverse hitting patterns, we implemented controlled random sampling on three critical joint axes:
 - Axis 3 (shoulder joint): Base angle of 15.0 degrees with random variation of ± 10.0 degrees
 - Axis 5 (elbow joint): Base angle of 60.0 degrees with random variation of ± 10.0 degrees
 - Axis 6 (wrist joint): Base angle of 0 degrees with random variation of ± 20.0 degrees
2. **Hitting Execution:** For each trial, the robotic arm would:
 - First, intercept the ball using the SONIC model’s prediction
 - Apply the randomly generated joint angles at the moment of contact
 - Execute the hitting motion to return the ball to the opponent’s side
3. **Outcome Recording:** We recorded whether the ball successfully landed on the opponent’s side of the table, along with the precise landing location.

This approach allowed us to collect data on effective hitting strategies while leveraging our previously established ball interception capabilities. By systematically varying the joint angles during the hitting phase, we were able to explore a wide range of possible returns, creating a comprehensive dataset that captures the relationship between joint movements and resulting ball trajectories.

D.2.2 Data Annotation Process

For data annotation, we used an Intel RealSense L515 camera to record the landing position of the ball. We divided the opponent’s side of the table into four quadrants (labeled A, B, C, and D) and encoded these landing zones using one-hot encoding. This encoded landing position information was incorporated as part of the input data, while the randomly sampled joint angles were used as labels. Using this structured dataset, we employed imitation learning techniques to train our IMPACT model, enabling it to learn the relationship between desired landing positions and the required joint movements to achieve them.

E Additional real-world experiments

We conducted extensive real-world experiments to validate the performance of our proposed system. To demonstrate the capabilities of our SpikePingpong model, we have included a demo.mp4 in the supplementary materials. This video showcases our system’s ability to return balls to different specified target locations on the opponent’s side of the table with high precision. Additionally, the video features human-robot interactive gameplay, highlighting the system’s responsiveness and adaptability in real-time competitive scenarios. These experiments confirm that our approach successfully integrates the neuromorphic vision-based ball-paddle contact detection with effective return stroke generation, resulting in a robust table tennis playing robot capable of controlled placement and responsive gameplay.